Inorganic Chemistry

Article

pubs.acs.org/IC

Synthesis, Characterization, and Reactivity of Furan- and Thiophene-Functionalized Bis(N-heterocyclic carbene) Complexes of Iron(II)

Julia Rieb,[†] Andreas Raba,[†] Stefan Haslinger,[†] Manuel Kaspar,[†] Alexander Pöthig,[†] Mirza Cokoja,[†] Jean-Marie Basset,[‡] and Fritz E. Kühn*[,†]

[†]Chair of Inorganic Chemistry/Molecular Catalysis, Catalysis Research Center, Technische Universität München, Ernst-Otto-Fischer-Straße 1, D-85747 Garching, Germany

[‡]Catalysis Center, King Abdullah University of Science and Technology (KAUST), Thuwal 23955-6900, Kingdom of Saudi Arabia

Supporting Information

ABSTRACT: The synthesis of iron(II) complexes bearing new heteroatom-functionalized methylene-bridged bis(N-heterocyclic carbene) ligands is reported. All complexes are characterized by single-crystal X-ray diffraction (SC-XRD), nuclear magnetic resonance (NMR) spectroscopy, and elemental analysis. Tetrakis(acetonitrile)-*cis*-[bis(*o*-imidazol-2-ylidenefuran)methane]iron(II) hexafluorophosphate (**2a**) and tetrakis(acetonitrile)-*cis*-[bis(*o*-imidazol-2-ylidenethiophene)methane]iron(II) hexafluorophosphate (**2b**) were obtained by aminolysis of [Fe{N(SiMe$_3$)$_2$}$_2$(THF)] with furan- and thiophene-functionalized bis(imidazolium) salts **1a** and **1b** in acetonitrile. The SC-XRD structures of **2a** and **2b** show coordination of the bis(carbene) ligand in a bidentate fashion instead of a possible tetradentate coordination. The four other coordination sites of these distorted octahedral complexes are occupied by acetonitrile ligands. Crystallization of **2a** in an acetone solution by the slow diffusion of Et$_2$O led to the formation of *cis*-diacetonitriledi[bis(*o*-imidazol-2-ylidenefuran)methane]iron(II) hexafluorophosphate (**3a**) with two bis(carbene) ligands coordinated in a bidentate manner and two cis-positioned acetonitrile molecules. Compounds **2a** and **2b** are the first reported iron(II) carbene complexes with four coordination sites occupied by solvent molecules, and it was demonstrated that those solvent ligands can undergo ligand-exchange reactions.

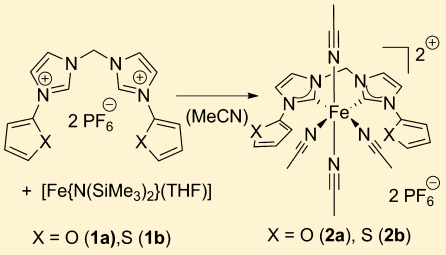

INTRODUCTION

Since their discovery 40 years ago and the isolation of the first free air-stable carbenes by Arduengo in the early 1990s, N-heterocyclic carbenes (NHCs) have been intensely studied.[1] Because of the good tunability of their electronic and steric properties, they quickly became an inherent part of the toolkit of organometallic chemistry.[2−4] In comparison to phosphines, which are soft ligands with a certain degree of π-back-bonding, the strong nucleophilic character of NHCs makes them more suitable as donor ligands for more electropositive transition metals such as iron.[4] However, the metal−carbene bond of these centers is thermodynamically weaker than that of late transition metals.[4,5] Additionally, evidence for kinetic instability of iron carbene complexes has been reported.[6] Therefore, an additional entropic stabilization by chelate effects is desirable in this case.

Fe-NHCs have been known since the 1970s, but in comparison to the extensive studies of coordination chemistry with late transition metals, the number of applications of Fe-NHC complexes is somewhat limited.[3,7,8] A widespread interest in these compounds was sparked only in the past decade. To date, most of the reported Fe-NHC complexes bear mono- or bis(carbene) motifs. Although polydentate NHCs offer greater possibility of electronic and steric tenability, only recently has a stronger focus been put on these ligands. In this regard, donor-substituted NHCs became very interesting targets. These ligands contain heteroatoms, which can act as additional donor atoms for metal coordination, resulting in potential bi-, tri-, tetra-, and pentadentate coordination. In most cases, nitrogen or oxygen are introduced into the ligand framework, but sulfur, phosphorus, and silicon can be considered as possible substituents as well.[9−13] Recently, we reported the synthesis and characterization of iron(II) complexes with tetradentate bis(N-heterocyclic carbene)bis(pyridine) (NCCN) ligands.[14] These air- and moisture-stable compounds also exhibit a number of interesting properties such activity in catalytic oxidation reactions.[15]

In this work, an introduction of pendant donor atoms such as oxygen and sulfur atoms into the chelating potentially tetradentate NHC ligands is described.

RESULTS AND DISCUSSION

Ligand Precursor Synthesis. The synthesis of bis(imidazolium) salts is based on the procedure previously published by the groups of Kühn and Wang.[14,16] Although CH_2Br_2 is used in excess, no monosubstituted products are observed due to the higher reactivity of the monosubstituted intermediate resulting from further electrophilic activation by the imidazolium substituent. The synthesis of the respective

Received: April 30, 2014
Published: September 4, 2014

   dx.doi.org/10.1021/ic500959m | Inorg. Chem. 2014, 53, 9598−9606

Scheme 1. Syntheses of the Imidazolium Salts 1a and 1b

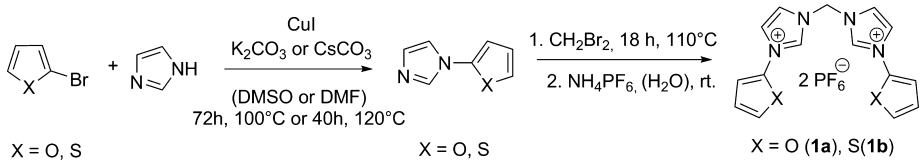

Scheme 2. Syntheses of Complexes 2a and 2b

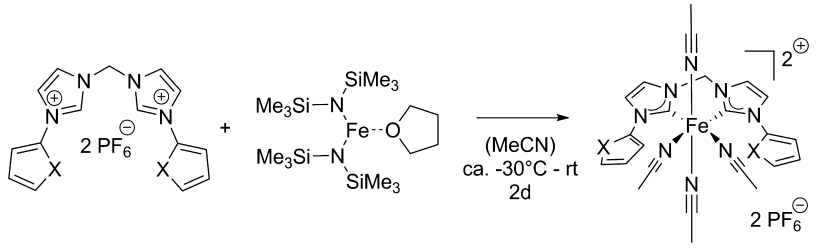

precursors for this reaction, 1-(furan-2-yl)-1*H*-imidazole and 1-(thiophen-2-yl)-1*H*-imidazole, is conducted by an Ullmann-type C−N coupling reaction using 2-bromofuran/2-bromothiophene and 1*H*-imidazole as the starting materials (see Scheme 1).[17−19]

The final step in the synthesis of bis(imidazolium) salts **1a** and **1b** is salt metathesis using a slight excess of ammonium hexafluorophosphate. The imidazolium salts could be obtained in high purity and good yields. Compounds **1a** and **1b** have not been reported previously and, therefore, they have been fully characterized by means of NMR spectroscopy, elemental analysis, and fast-atom-bombardment mass spectrometry (FAB-MS; for details, see the Experimental Section and Supporting Information, SI). Imidazolium salt **1a** was also analyzed by single-crystal X-ray diffraction (SC-XRD). The molecular structure of **1a**, which crystallizes in the orthorhombic space group *Pnma*, is shown in Figure S4 (see the SI). All distances and angles are comparable to the related bis(imidazolium) derivatives reported in the literature.[20]

Synthesis and Characterization of Fe-NHC Complexes 2a and 2b. The cationic iron(II) complexes **2a** and **2b** were prepared by aminolysis of $[Fe\{N(SiMe_3)_2\}_2{\cdot}THF]$ (THF = tetrahydrofuran) with the ligand precursors **1a** and **1b** in acetonitrile at −35 °C (see Scheme 2). The preparation procedure is based on a previously described synthesis of iron(II) complexes with bis(N-heterocyclic carbene) ligands by Danopoulos et al.[9] and Kühn et al.[14] In this reaction, bis(trimethylsilyl)amide deprotonates the imidazolium salt, generating a free carbene, which then coordinates to the iron(II) center. The byproduct bis(trimethylsilyl)amine is removed in vacuo along with the solvent. A variety of examples exist in the literature, demonstrating the generation of Fe^{II}-NHC complexes from the iron bis(amide) precursor and imidazolium salts with weakly coordinating anions.[8,14,21] However, Danopoulos et al.[22] demonstrated that under certain conditions a coordinating halide facilitates deprotonation, whereas imidazolium salts associated with weakly coordinating anions are unreactive, yet this has been shown only for bulky monoimidazolium salts in weakly coordinating solvents.

The crude product for both complexes is a brown solid, which can be purified by the stepwise addition of diethyl ether, leading to precipitation of **2a** as a bright-orange solid and **2b** as a dark-orange solid, respectively. Both products are sensitive to moisture and decompose in air after several hours.

Spectroscopic Characterization of 2a and 2b. All obtained complexes are diamagnetic and therefore suitable for NMR spectroscopy. The absence of imidazolium protons in the ^{1}H NMR spectrum of **2a** implies deprotonation of the ligand precursor (Figure 1). There is also only one set of signals for

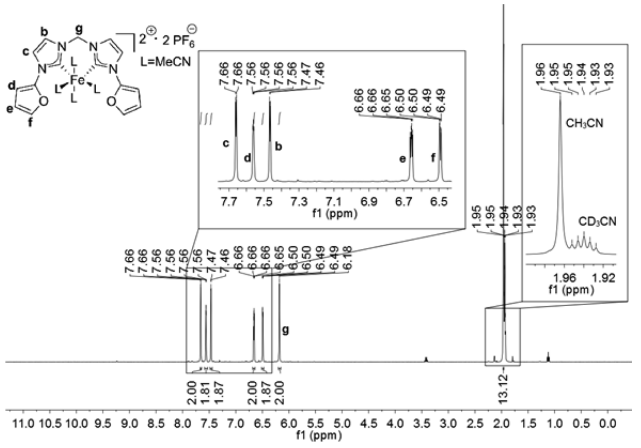

Figure 1. ^{1}H NMR spectrum of complex **2a** in CD_3CN.

imidazole backbone protons as well as for the furan moieties, which could indicate a possible symmetric coordination of the imidazolylidene ligand to the iron(II) center. The signals at 7.66 and 7.47 ppm are attributed to the two imidazole backbone protons because they both appear as doublets and display the same vicinal coupling constant of $^3J_{HH}$ = 2.0 Hz, which is common for the backbone protons of imidazolium compounds.[14] The signals at 7.56, 6.65, and 6.48 ppm, which show a long-range coupling pattern in addition to vicinal coupling, can be assigned to the protons of the furan moiety. The remaining singlet at 6.17 ppm is attributed to the protons of the methylene bridge. Deprotonation of the ligand precursor forming a NHC is also displayed in the ^{13}C NMR spectrum, showing a signal at 196.06 ppm, which is typical for a carbene carbon, lying in the usual range (210−190 ppm) for iron(II) carbene complexes (for the spectrum, see the Supporting Information).[13,14,23−25]

dx.doi.org/10.1021/ic500959m | *Inorg. Chem.* 2014, 53, 9598−9606

After purification, the ^{1}H NMR spectrum of compound **2a** shows a clear presence of 4 equiv of free acetonitrile molecules. Coordination of four MeCN molecules to the iron center could explain this observation. Because of rapid exchange with the deuterated solvent, nondeuterated acetonitrile molecules cannot be observed as ligated molecules.

Because the ligand systems **1a** and **1b** are isostructural, it was expected that they display the same chemical behavior toward the iron precursor. Indeed, the ^{1}H NMR spectrum of **2b** (Figure 2) looks very similar to the spectrum of compound **2a**.

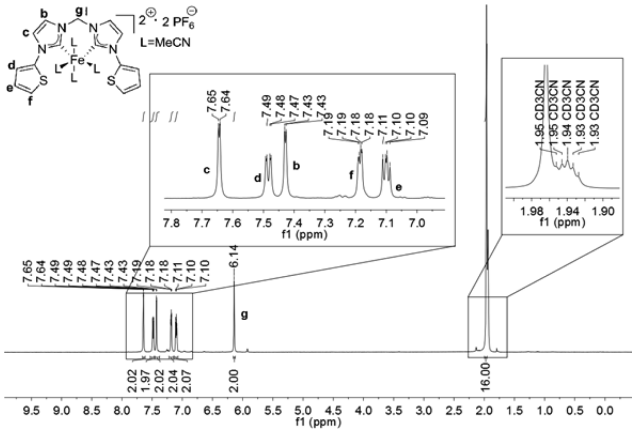

Figure 2. ^{1}H NMR spectrum of **2b** in CD_3CN.

As was already discussed for compound **2a**, the absence of the imidazolium protons and the presence of only one set of signals indicate a symmetrical coordination to the iron(II) center. Both backbone imidazolylidene protons appear as doublets at 7.64 and 7.43 ppm, respectively, with the expected low vicinal coupling constant of 2.1 Hz. In the thiophene moiety, not only vicinal coupling but also a long-range coupling over four bonds can be observed. The methylene-bridged protons appear as a singlet at 6.14 ppm. The ^{13}C NMR spectrum of compound **2b** (see the SI) displays a typical shift of the carbene carbon coordinated to the iron(II) center (192.85 ppm).[13,14,23−25]

SC-XRD Structure Analysis of Compounds 2a and 2b. In order to further elucidate the structure of the synthesized compounds, SC-XRD experiments were performed. The single crystals of **2a** were grown via the slow diffusion of diethyl ether in an acetonitrile solution of a crude product and were obtained as bright-orange fragments. The collected data reveal a bidentate coordination of the bis(N-heterocyclic carbene) ligand and coordination of four acetonitrile molecules to the remaining coordination sites (see Figure 3).

This compound crystallizes in trigonal space group $P3_1c$. To the best of our knowledge, **2a** is the first reported iron(II) carbene complex with four coordination sites occupied only by solvent molecules.

Both Fe−C_{NHC} bond lengths of **2a** are nearly equally long [1.943(5) to 1.950(5) Å (in the two symmetry-independent molecules)] and lie within the expected range for octahedral cationic methylene-bridged iron bis(carbene) complexes (1.84−1.99 Å).[14,26] Compared to the reported series of neutral bidentate or monodentate bis(carbene)iron(II) dihalide complexes (Fe−C = 2.07−2.13 Å), the Fe−C distances in **2a** are definitely shorter, which is certainly due to the cationic nature of **2a**.[26,27] On the other hand, in comparison to the Fe−NHC bond length in cationic tetradentate methylene-bridged NCCN

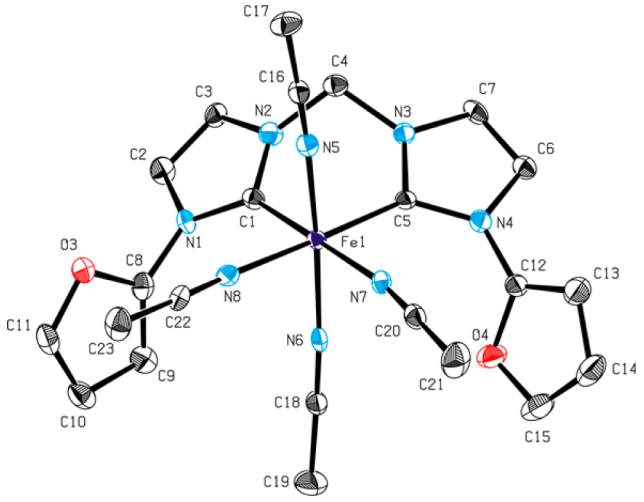

Figure 3. ORTEP view of one independent molecule of the cationic complex **2a** displaying vibrational ellipsoids at 50% probability. Hydrogen atoms as well as the PF_6^- anion and cocrystallized acetonitrile molecules are omitted for clarity.

complexes with two pyridine moieties as nitrogen donors reported by our group [1.837(2) Å], the Fe−C distances in **2a** are significantly longer.[14] A greater σ-donor ability of acetonitrile compared to the π-acceptor ability of pyridine results in a longer iron−carbene bond for NHC coordination trans to acetonitrile compared to trans to pyridine. This effect is also pronounced in propylene-bridged cationic tetradentate NCCN iron(II) complexes reported by Kühn et al.[14] In this complex, the introduction of a propylene bridge between two imidazole moieties results in cis coordination of acetonitrile molecules and therefore in different Fe−C distances because one NHC is coordinated trans to acetonitrile [Fe−C = 1.913(2) Å] and one to pyridine [Fe−C = 1.897(2) Å].[14]

The bond lengths between iron and nitrogen atoms of acetonitrile ligands in **2a** vary slightly. The distances to axial acetonitrile molecules are shorter than those to the equatorial ones [1.938(5)/1.924(5) Å vs 1.970(4)/1.975(5) Å (or 1.934(5)/1.938(5) Å vs 1.999(5)/1.999(5) Å for the second independent molecule)]. This could be due to the strong trans influence of NHCs or due to increased steric hindrance along the equatorial plane.[26] The bond angles on the equatorial plane differ more from the ideal 90° for an octahedral coordination than the angles between the equatorial and axial planes (see Table 1). Probably the steric demands and geometry of the OCCO ligand dictate this minor anomaly. In comparison, the *trans*-[Fe(NCCN)^{Me}(MeCN)$_2$] complex displays even a significantly smaller C−Fe−C angle of 85.85°.[14]

It was possible to crystallize complex **2b** by the slow diffusion of diethyl ether into a saturated solution of **2b** in acetonitrile, and single crystals in the form of bright-orange fragments were obtained. Complex **2b** crystallizes in the monoclinic space group $P2_1/n$. In analogy to complex **2a**, X-ray analysis revealed a distorted octahedral complex with coordination of the bis(N-heterocyclic carbene) ligand in a bidentate manner and occupation of the remaining sites by four acetonitrile molecules (Figure 4). The relevant bond lengths and angles of **2b** lie in the same range and follow the same trends as those for **2a** (see Table 1). Because Fe−C distances are very similar for **2a** and **2b**, it is obvious that furan or thiophene substitution does not have a significant influence on the strength of iron−carbene bonding.

dx.doi.org/10.1021/ic500959m | *Inorg. Chem.* 2014, 53, 9598−9606

Table 1. Selected Bond Lengths [Å] and Bond Angles [deg] of 2a (two independent molecules) and 2b

atom groups	2a	2b	atom groups	2a	2b
Fe1−C1	1.946(5)/1.943(7)	1.951(3)	N7−Fe1−N8	86.88(17)/85.8(2)	85.59(8)
Fe1−C5	1.950(5)/1.943(5)	1.950(2)	C1−Fe1−N5	91.5(2)/90.1(2)	91.61(9)
Fe1−N5	1.938(5)/1.934(8)	1.940(2)	C5−Fe1−N5	90.9(2)/91.1(2)	89.82(9)
Fe1−N6	1.924(5)/1.938(5)	1.912(2)	N7−Fe1−N5	89.6(2)/87.7(2)	84.23(8)
Fe1−N7	1.970(4)/1.999(5)	1.984(2)	N5−C16−C17	177.7(6)/178.6(6)	179.3(3)
Fe1−N8	87.9(2)/87.7(2)	1.989(2)	N6−C18−C19	178.3(6)/178.8(6)	179.3(3)
C1−Fe1−C5	87.9(2)/87.7(2)	87.67(10)	N7−C20−C21	179.1(7)/179.4(6)	178.4(3)
C5−Fe1−N7	91.6(2)/93.9(2)	93.39(9)	N8−C22−C23	178.3(6)/179.3(7)	179.7(3)

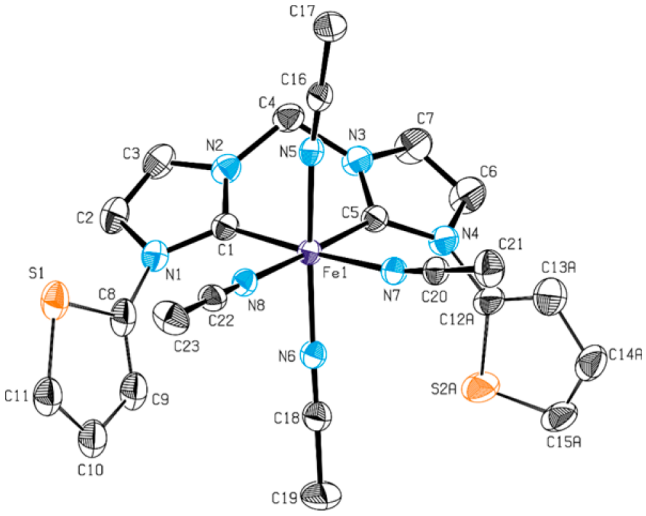

Figure 4. ORTEP view of cationic complex 2b displaying vibrational ellipsoids at 50% probability. Hydrogen atoms as well as the PF_6^- anions are omitted for clarity.

Because coordination of the oxygen and sulfur heteroatoms to the iron center was not observed, three possible explanations for this behavior were considered. First, the coordination ability of acetonitrile is too great in comparison to the oxygen in the furan moiety or the sulfur in thiophene. Gibson et al. studied the reactions of bis(imino)furan and bis(imino)thiophene ligands with $FeCl_2$.[28] No coordination has been observed in this case, confirming that oxygen and sulfur atoms are rather poor donors in these systems. The second reason could be that the ring strain for a possible coordination in a tetradentate manner prevents formation of the desired complex. For the tetradentate complex *trans*-$[Fe(NCCN)^{Me}(MeCN)_2]$ reported by Kühn et al.,[14] the equatorial bond angles of C−Fe−C [85.85(9)°] and C−Fe−N [79.45(7)°] were already quite far away from a perfect octahedral geometry (90°), proving a significant ring strain even for the pyridyl motif, which should be less strained compared to a five-membered heterocycle moiety. By applying bis(imino)-N-heterocyclic carbene ligands of the type bis[(DIPP)N═C(Me)](NHC) (DIPP = 2,6-diisopropylphenyl), Al Thagfi and Lavoie[11] and Byers et al.[12] demonstrated that their ligands coordinated unexpectedly in a bidentate fashion instead of the desired tridentate fashion. In both cases, a tridentate binding with a five-membered heterocyclic framework was proposed to be geometrically too constrained to coordinate in the desired manner. It is suggested that, in contrast to bis(imino)-N-heterocyclic carbene systems, bis(carbene)pyridine ligands coordinate in a tridentate fashion as a results of the observed bond angles associated with a six-membered pyridine ring, the excellent σ-donating ability of carbene ligands, and the cationic charge of the respective complexes.[12] Interestingly, by substituting imidazole with pyrimidine as the source of the NHC moiety in the bis(imino)-N-heterocyclic carbene ligands, Byers and co-workers were able to isolate the desired iron complex bearing the ligand in a tridentate fashion.[12] Again, it seems that the bond angles associated with the six-membered pyrimidine ring relieve some of the geometric strain and thus allow the desired coordination. Finally, an aromatic behavior of the furan and thiophene moieties may thermodynamically preclude coordination to an iron center.

To exclude the first possibility, another batch of crystals of complex **2a** was grown from a solution in acetone and THF by the slow diffusion of Et_2O. The bright-yellow single crystals of compound **3a** obtained from a solution of **2a** in acetone crystallized in the triclinic space group $P\bar{1}$. Unexpectedly, the molecular structure displayed a distorted octahedral coordination by two bidentate NHC ligands and two cis-positioned acetonitrile molecules (see Figure 5), whereas coordination of

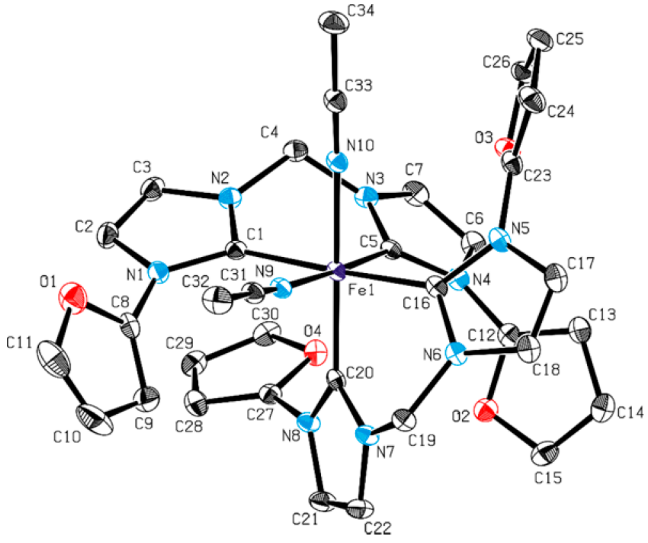

Figure 5. ORTEP view of the cationic complex 3a obtained from a solution of compound 2a in acetone, showing the vibrational ellipsoids at the 50% probability level. PF_6^-, hydrogen atoms, and cocrystallized acetone molecules are omitted for clarity. Selected bond lengths [Å] and bond angles [deg]: Fe1−C1 1.964(3), Fe1−C5 1.921(3), Fe1−C16 1.966(3), Fe1−C20 1.927(3), Fe1−N9 1.967(3), Fe1−N10 1.970(3); C1−Fe1−C5 88.37(12), C16−Fe1−N9 87.49(11), C5−Fe1−C16 92.40(12), C1−Fe1−N10 87.44(11), C5−Fe1−N10 92.73(11), C16−Fe1−N10 89.60(12), N9−Fe1−N10 84.61(10), C1−Fe1−C20 94.64(12), C5−Fe1−C20 90.82(12), C16−Fe1−C20 88.28(12), N9−Fe1−C20 91.84(11), N10−C33−C34 179.5(4), N9−C31−C32 179.3(4).

dx.doi.org/10.1021/ic500959m | Inorg. Chem. 2014, 53, 9598−9606

acetone was not observed. The formation of tetracoordinate 14-valence-electron iron(II) complexes is unfavorable in this case because of the instability of low-spin d^6 iron compounds with nonelectrostatic interaction between the metal and not particularly bulky ligands. Yet, it seems that, despite the lack of an excess of strongly coordinating solvent molecules, the furan-functionalized bis(carbene) ligand still coordinates in a bidentate manner. A formation of green-brown precipitate in the crystallization batch was observed, containing decomposition products. A formation of similar complexes was observed by Meyer et al.[26] in a reaction of the iron precursor with the respective bis(imidazolium) salts with small substituents such as methyl and ethyl groups.

The bond lengths between iron and carbene carbons vary slightly and lie within the expected range for iron tetrakis- and tetracarbene complexes.[21,26,29] Fe−C distances trans to MeCN are in the range of 1.92−1.93 Å, and those in the cis position are slightly longer (1.96−1.97 Å). This fact reflects a strong trans influence of NHCs. The iron complex with a cyclic tetracarbene ligand synthesized by Meyer et al.[26] displays the same distribution: the distances trans to MeCN are in the range 1.92−1.95 Å, while those trans to another carbene were in the range 1.96−1.99 Å. Compared to the macrocyclic tetracarbene iron(II) complexes reported by the groups of Meyer and Jenkins, the Fe−C distances overall are slightly shorter for the obtained compound **3a**.[21,29] This fact also reflects a strong trans influence of carbenes as well as constrained geometry of macrocyclic tetracarbene ligands.

The distances from the iron(II) center to the nitrogen atoms of the acetonitrile ligands in **3a** [1.967(3) Å and 1.970(3) Å, respectively] are in the same range as the Fe−N distances in **2a** for equatorially positioned acetonitrile molecules, reflecting the increased electron density on the iron center as well as steric demand of two bis(carbene) ligands. The distances for two acetonitrile ligands of Meyer's tetracarbene complex lie in the same range as that for **3a** [1.972(5)−1.983(4) Å].[26] The Fe−N distances for the macrocyclic complex by Cramer and Jenkins[29] are in the range 1.93−1.92 Å and therefore are rather similar to the tetradentate complexes reported by Kühn et al.[14]

The bond angles between iron and two tethered carbene carbons for **3a** are 88.28(12)° and 88.37(12)° for C16−Fe−C20 and C1−Fe−C5, respectively. The angles are slightly bigger than those for the comparable complex reported by Meyer et al., which amount to 86.6° and 86.9°.[26] In comparison to **2a**, the C−Fe−C angle of **3a** is only marginally larger in spite of increased steric demand.

The crystals of **3a** grown from a solution of **2a** in THF could also be determined by SC-XRD. Although these crystals were of inferior quality, the data could be refined to a stage at which the principle constitution can be proven. The preliminary analysis revealed also the same distorted octahedral coordination by two bidentate bis(N-heterocyclic carbene) ligands and two cis-coordinated acetonitrile molecules. As in the case of the furan-functionalized iron(II) OCCO bis(carbene) complex **2a**, a crystallization of **2b** from acetone and THF was attempted. As in the case of **3a**, a precipitation of decomposition products is observed. Unfortunately, the bright-yellow crystals grown in acetone by the slow diffusion of Et_2O were not suitable for X-ray diffraction. To date, it has not been possible to obtain crystals of **3b** suitable for SC-XRD. To exclude the possibility of a competition between the solvent molecules and the furan and thiophene moieties, a complexation reaction in THF was attempted. As expected, the imidazolium salts **1a** and **1b** were insoluble in this solvent. The reaction mixtures were stirred at room temperature for 4 days and then evaporated to dryness. The obtained solids were insoluble in both CH_2Cl_2 and dimethyl sulfoxide (DMSO), but they dissolved in acetone, yielding brown-orange solutions. The ^{1}H NMR spectrum revealed the predominant presence of the respective free ligand precursors.

There are also some minor signals that might represent additional products. Compared to the signals of the non-deprotonated imidazolium salt, these are shifted upfield, which was already observed for the other complexes. However, the low intensity of these signals does not allow one to draw any justifiable conclusions on the structure of possible additional products. These observations are in accordance with the studies on aminolysis reactions of $[Fe\{N(SiMe_3)_2\}_2\cdot THF]$ with imidazolium salts associated with noncoordinating anions in THF reporting the formation of intractable mixtures of products in these cases.[22]

Ligand-Exchange Experiments. In order to explore the ability of the four MeCN solvent ligands to undergo ligand-exchange reactions, **2a** was treated with trimethylphosphine and 1,2-bis(dimethylphosphanyl)ethane (dmpe). In an NMR-scale reaction, a 1 M solution of PMe_3 in THF was added stepwise in stoichiometric amounts to a solution of **2a** in MeCN-d_3 at room temperature. The chosen steps for the addition of PMe_3 were 1, 2, 3, 4, and 10 equiv, respectively, and after each step, both ^{1}H and ^{31}P NMR spectra were recorded. After the addition of 1 equiv of PMe_3, the ^{31}P NMR spectrum shows a distinct signal at 29.28 ppm, which is assigned to a monosubstituted derivative of **2a** (see Figure 6). ^{1}H NMR (see the SI and also for all other steps that are discussed) confirms this assignment.

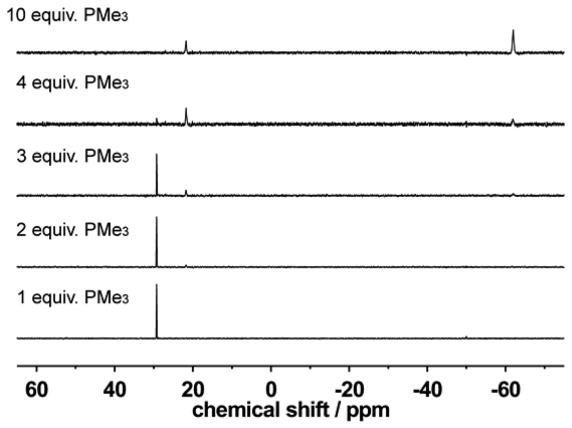

Figure 6. ^{31}P NMR spectra of the reaction of **2a** with 1, 2, 3, 4, and 10 equiv of PMe_3 in MeCN-d_3 at room temperature. Three signals are shown: 29.28 ppm (monosubstituted complex), 21.72 ppm (tetrasubstituted complex), and −61.98 ppm (free PMe_3).

The further addition of a second and third 1 equiv of PMe_3 did not result in the formation of di- or trisubstituted derivatives, as seen in ^{1}H NMR (see the SI) and ^{31}P NMR (Figure 6). Interestingly, a second species is formed in both cases, exhibiting a signal at 21.72 ppm in the ^{31}P NMR spectrum. On the basis of the integral ratio in ^{1}H NMR, this species is identified as the tetrasubstituted derivative of **2a**, bearing four PMe_3 ligands in addition to the chelating bis(carbene) ligand. Apparently, formation of the mono- and tetrasubstituted derivatives is thermodynamically favored. With

dx.doi.org/10.1021/ic500959m | Inorg. Chem. 2014, 53, 9598−9606

the addition of a fourth 1 equiv of PMe_3, the ^{31}P signal at 29.28 ppm diminishes almost completely and the tetrasubstituted species exists exclusively. Further excess of trimethylphosphine did not result in any subsequent reactions, as shown by the detection of free PMe_3 in both ^{31}P and ^{1}H NMR.

In order to reveal the nature of the monosubstituted derivative, namely, whether the phosphine is coordinated cis or trans to the NHC ligand, density functional theory (DFT) calculations were conducted in order to energetically compare all three possible isomers (**A**, trans to NHC; **B**, cis to NHC and directing away from the methylene bridge; **C**, cis to NHC and directing toward the methylene bridge). If the energies are examined relative to **A** (0 kcal/mol), **B** is stabilized by 1 kcal/mol whereas **C** is destabilized by 3 kcal/mol. Although the differences in energies are relatively small, a preferred coordination of one PMe_3 cis to NHC and directing away from the methylene bridge seems evident (**B**). This is confirmed by ^{1}H NMR spectroscopy, where the signal for the methylene bridge at 6.17 ppm for **2a** splits up drastically after the addition of 1 equiv of PMe_3 into two doublets at 6.39 and 5.53 ppm. One would expect such an observation for cis coordination of PMe_3 because both protons of the methylene backbone are not chemically identical anymore, leading to an individual set of signals for each of the two protons. When the ^{1}H NMR and DFT data are combined, it is evident that in the case of the monosubstituted derivative of **2a** the PMe_3 ligand is coordinated cis to NHC in fashion **B**. In this context, Driess et al.[30] recently reported on the isolation of an iron(II) complex featuring bis[*N*-(2,6-diisopropylphenyl)imidazol-2-ylidene]-methylene and the PMe_3 ligand mutually coordinated to the metal center. Remarkably, in this complex, one of the two coordinated PMe_3 molecules undergoes an intramolecular C−H bond activation of one of the phosphorus-bound methyl groups. In the case of the PMe_3 substitution reactions with **2a**, we did not observe similar reactivity.

Ligand-exchange reactions of **2a** with the possibly chelating ligand dmpe on an NMR scale at room temperature showed that a mixture of different products as well as a free ligand precursor is existing under Schlenk conditions in a MeCN-d_3 solution (for the respective ^{1}H, ^{13}C, and ^{31}P NMR, see the SI). Assignment of the signals was not possible based on the collected data. However, crystallization by the slow diffusion of diethyl ether into the reaction solution gave orange crystals, which were identified by SC-XRD as $[Fe(dmpe)_2(MeCN)_2]$ (for the single-crystal X-ray structure, see the SI), a compound that has been known for quite some time, including the molecular structure determined by X-ray diffraction.[31] Keeping in mind that the iron−carbene bond can be kinetically unstable under certain conditions (see above), a chelating phosphine as the ligand could lead to loss of the carbene ligand, which makes chelating phosphines undesirable reaction partners for ligand-exchange reactions for such iron complexes.

Attempts to broaden the scope in terms of neutral ligands for solvent ligand replacement, carbon monoxide was considered as a suitable candidate, especially because it exhibits strong π-acceptor properties in contrast to the σ-donor ability of PMe_3. Unfortunately, no defined reaction products could be obtained, and the reaction mixture became paramagnetic, which indicates the presence of either iron(III) or high-spin iron(II) species.

CONCLUSIONS

The synthesis of new bis(carbene)iron(II) complexes **2a** and **2b** coordinated by a furan- or thiophene-modified bis(carbene) ligand and four acetonitrile ligands is reported. The obtained compounds were characterized, and their molecular structure was confirmed by SC-XRD. Compound **2a** transforms into the bis(carbene)iron(II) complex **3a** upon dissolution in acetone and growing crystals by the slow diffusion of diethyl ether into this solution. **3a** is coordinated by two bis(NHC) ligands and two cis-positioned acetonitrile molecules. Because of four accessible coordination sites, the new bis(carbene) complexes **2a** and **2b** as well as any similar aryl-substitued bis(carbene) complexes may be applicable as starting materials for the synthesis of other iron complexes or iron clusters. The ability of the acetonitrile ligands to undergo ligand-exchange reactions was examined. The addition of PMe_3 in stepwise stoichiometric amounts led to the substitution of either one or four MeCN ligands, whereas di- and trisubstituted derivatives were not observed. Ligand-exchange reaction with dmpe indicates possible kinetic instability of the Fe−C bond. Further examinations on the Fe−C bond stability as well as subsequent reactivity are under current investigation in our laboratories.

EXPERIMENTAL SECTION

Materials. Unless otherwise stated, all syntheses were carried out under an argon atmosphere using standard Schlenk and glovebox techniques. The solvents were dried via a MBraun MB SPS purification system and when necessary degassed by three freeze−pump−thaw cycles and stored over 3 Å molecular sieves. Additionally, acetonitrile was refluxed over phosphorus pentoxide at least for 3 h and distilled prior to use. All chemicals were purchased from common commercial suppliers and used without further purification. $[Fe\{N(SiMe_3)_2\}_2\cdot THF]$ and 2-bromofuran were synthesized according to literature procedures.[32,33] The syntheses of 1-(furan-2-yl)imidazole and 1-(thiophen-2-yl)imidazole are based on modified procedures described by Zhang, Chen, and You.[18,19,34]

Instruments. NMR spectra were recorded on a Bruker Avance DPX 400 spectrometer (^{1}H NMR, 400.13 MHz; ^{13}C NMR, 100.53 MHz), and chemical shifts are reported relative to the residual signal of the deuterated solvent. NMR spectra were analyzed using *MestReNova* (version 8.0.0-10524; Mestrelab Research SL, Escondido, CA). Elemental analyses (C/H/N) were obtained by the microanalytical laboratory at the Technical University of Munich. FAB-MS data were collected with a Finnigan MAT 90 spectrometer.

Computational Studies. All calculations were performed with *Gaussian 09*[35] using the DFT/Hartree−Fock hybrid model Becke3LYP.[36] For geometry optimizations, the split-valence double-ζ basis set 6-31G(d) was used for all atoms.[37] Solvation effects were taken into account by using the polarizable continuum model solvation model with acetonitrile as the solvent.[38] No symmetry or internal-coordinate constraints were applied during optimization. All reported ground states were verified as being true minima by the absence of negative eigenvalues in vibrational frequency analysis. *xyz* coordinates for all calculated compounds can be found in the SI. Single-point calculations on all optimized structures were performed to ensure energy convergence by using the triple-ζ basis set 6-311++G(d,p) on all atoms.[39]

Single-Crystal X-ray Structure Determination. Data were collected on single-crystal X-ray diffractometers (Kappa Apex II-D8 and Kappa Apex II-FR591, both from Bruker) equipped with CCD detectors (Bruker APEX II, κ-CCD), a fine-focus sealed tube with graphite monochromator (Kappa Apex II-D8), or a rotating anode FR591 with MONTEL optic (Kappa Apex II-FR591), using Mo Kα radiation (λ = 0.71073 Å), and the *APEX 2* software package.[40] Measurements were performed on a single crystal coated with perfluorinated ether, which was fixed on the top of a glass capillary and frozen at 123 K under a stream of cold nitrogen. A matrix scan was used to determine the initial lattice parameters. Reflections were merged and corrected for Lorentz and polarization effects, scan speed, and background using *SAINT*.[41] Absorption corrections, including

dx.doi.org/10.1021/ic500959m | *Inorg. Chem.* 2014, 53, 9598−9606

Table 2. Crystallographic Data for Compounds 1a, 2a, 2b, and 3a

	1a	2a	2b	3a
formula	$C_{17}H_{17}F_{12}N_5O_2P_2$	$C_{25}H_{27}F_{12}FeN_9O_2P_2$	$C_{23}H_{24}F_{12}FeN_8P_2S_2$	$C_{40}H_{42}F_{12}FeN_{10}O_6P_2$
fw	613.30	831.34	822.43	1104.63
color/habit	yellow/fragment	red-orange/block	red-orange/fragment	yellow/fragment
cryst dimens [mm^3]	0.13 × 0.23 × 0.41	0.440 × 0.465 × 0.475	0.430 × 0.538 × 0.582	0.29 × 0.46 × 0.67
cryst syst	orthorhombic	trigonal	monoclinic	triclinic
space group	*Pnma* (No. 62)	$P3_1c$ (No. 159)	$P2_1/n$ (No. 14)	$P\bar{1}$ (No. 2)
a [Å]	24.2220(9)	20.6829(3)	13.0550(3)	12.0827(3)
b [Å]	14.0397(6)	20.6829(2)	14.3291(3)	14.0187(4)
c [Å]	6.9906(3)	27.1011(5)	18.8249(4)	14.1427(4)
α [deg]	90	90	90	81.3220(10)
β [deg]	90	90	95.920(1)	77.0820(10)
γ [deg]	90	120	90	82.1540(10)
V [$Å^3$]	2377.29(17)	10040.2(4)	3502.73(13)	2295.02(11)
Z	4	12	4	2
T [K]	123(2)	123(2)	123(2)	123(2)
D_{calcd} [g cm^{-3}]	1.714	1.650	1.560	1.599
μ [mm^{-1}]	0.304	0.654	0.734	0.506
$F(000)$	1232	5040	1656	1128
θ range [deg]	1.68 to 25.47	0.75 to 25.49	1.79 to 25.39	1.74 to 25.44
index ranges (h, k, l)	±29, ±16, ±8	±24, ±24, ±32	±15, ±17, ±22	±14, ±16, ±17
no. of reflns collected	41103	306292	111677	74023
no. of indep reflns/R_{int}	2292/0.0689	12376/0.0392	6439/0.0203	8462/0.033
no. of obsd reflns [$I > 2\sigma(I)$]	1935	11787	6002	7189
no. of data/restraints/param	2292/0/188	12376/158/955	6439/484/656	8462/87/747
R1/wR2 [$I > 2\sigma(I)$][a]	0.0264/0.0651	0.0429/0.1145	0.0417/0.1040	0.0496/0.1283
R1/wR2 (all data)[a]	0.0355/0.0700	0.0455/0.1171	0.0448/0.1070	0.0592/0.1361
GOF (on F^2)[a]	1.043	1.058	1.038	1.038
largest diff peak and hole [e $Å^{-3}$]	+0.244/−0.285	+1.037/−0.623	+0.839/−0.546	+1.494/−0.743

[a] $R1 = \sum(||F_o| - |F_c||)/\sum|F_o|$; $wR2 = \{\sum[w(F_o^2 - F_c^2)^2]/\sum[w(F_o^2)^2]\}^{1/2}$; $GOF = \{\sum[w(F_o^2 - F_c^2)^2]/(n - p)\}^{1/2}$.

odd- and even-ordered spherical harmonics, were performed using *SADABS*.[41] Space-group assignments were based upon systematic absences, E statistics, and the successful refinement of the structures, and the respective data are shown in Table 2. Structures were solved by direct methods with the aid of successive difference Fourier maps[40] and refined against all data using *SHELXL-97* and *SHELXL-2013* in conjunction with *SHELXL*.[42] If not mentioned otherwise, non-hydrogen atoms were refined with anisotropic displacement parameters and hydrogen atoms were placed in ideal positions using the *SHELXL* riding model. Full-matrix least-squares refinements were carried out by minimizing $\sum w(F_o^2 - F_c^2)^2$ with the *SHELXL-97*/*SHELXL-2013* weighting scheme. Neutral atom scattering factors for all atoms and anomalous dispersion corrections for the non-hydrogen atoms were taken from the *International Tables for Crystallography*.[43] Images of the crystal structures were generated by *PLATON*.[44] Crystallographic data for the structures reported in this paper have been deposited with the Cambridge Crystallographic Data Centre (CCDC 997386−997389). Copies of the data can be obtained free of charge from CCDC, 12 Union Road, Cambridge CB2 1EZ, U.K. [fax (+44)1223-336-033; e-mail deposit@ccdc.cam.ac.uk].

Synthesis Procedures. *General Procedure for (Methylene-Bridged) Imidazolium Salts.* 1-(Furan-2-yl)imidazole (719 mg, 5.4 mmol) or 1-(thiophen-2-yl)imidazole (1.87 g, 12.5 mmol) was dissolved in an excess of 1,2-dibromomethane and refluxed at 110 °C for 18 h. The remaining CH_2Br_2 was removed in vacuo, and the precipitate was then dissolved in methanol. The products were obtained after precipitation with diethyl ether. The solids were separated from the solution by filtration, washed with diethyl ether (3 × 5 mL), and dried in vacuo. Subsequently, the bromide salts were dissolved in water, and an aqueous solution of ammonium hexafluorophosphate (2.5 mol equiv) was added to the stirred solution to form a precipitate, which was filtered off, washed with water (4 × 3 mL), and dried in vacuo.

*3,3′-Methylenebis(1-furan-2-yl)-1H-imidazolium Hexafluorophosphate (**1a**).* The compound was obtained as a colorless solid. Yield: 75%. ^{1}H NMR (400 MHz, DMSO-d_6, 300 K): δ 10.01 (t, $^4J_{HH}$= 1.6 Hz, $2H_{im}$, NC*H*N), 8.38 (t, $^3J_{HH} \approx {}^4J_{HH}$ = 1.9 Hz, $2H_{im}$), 8.20 (t, $^3J_{HH} \approx {}^4J_{HH}$ = 1.8 Hz, $2H_{im}$), 7.91 (m, $2H_{Fu}$), 6.99 (d, $^3J_{HH}$ = 3.5 Hz, $2H_{Fu}$), 6.82 (dd, $^3J_{HH}$= 3.4 Hz, $^3J_{HH}$ = 2.0 Hz, $2H_{Fu}$), 6.76 (s, 2H, NCH_2N). ^{13}C{^{1}H} NMR (101 MHz, DMSO-d_6, 300 K): δ 142.24 (CCH_2CH_2), 140.47 (NCO), 136.49 (NCHN), 123.24 (C_{im}), 120.56 (C_{im}), 112.71 (CH$_2$*C*H$_2$CH$_2$), 100.64 (CH$_2$*C*H$_2$O), 58.94 (NCH_2N). Anal. Calcd: C, 31.48; H, 2.47; N, 9.79. Found: C, 31.43; H, 2.42; N, 9.66. FAB-MS ([M]$^+$): m/z 424.1 ([**1a** − 1PF_6^-]$^+$).

*3,3′-Methylenebis(1-thiophen-2-yl)-1H-imidazolium Hexafluorophosphate (**1b**).* The product was obtained as a gray solid. Yield: 74%. ^{1}H NMR (400 MHz, DMSO-d_6, 300 K): δ 9.94 (t, $^4J_{HH}$ = 1.6 Hz, 2H, NC*H*N), 8.36 (t, $^3J_{HH} \approx {}^4J_{HH}$ = 1.8 Hz, 2H, H_{im}), 8.20 (t, $^3J_{HH} \approx {}^4J_{HH}$ = 1.8 Hz, 2H, H_{im}), 7.73 (dd, $^3J_{HH}$= 5.5 Hz, $^4J_{HH}$ = 1.5 Hz, 2H, H_{Th}), 7.59 (dd, $^3J_{HH}$ = 3.8 Hz, $^4J_{HH}$ = 1.5 Hz, 2H, H_{Th}), 7.22 (dd, $^3J_{HH}$ = 5.4 Hz, $^3J_{HH}$ = 3.8 Hz, 2H, H_{Th}), 6.72 (s, 2H, NCH_2N). ^{13}C{^{1}H} NMR (101 MHz, DMSO-d_6, 300 K): δ 138.19 (NC*H*N), 134.70 (NCS), 126.96 (CH*C*HCH), 126.30 (CCHCH), 123.31 (C_{im}), 123.14 (CH*C*HS), 123.03 (C_{im}), 58.79 (NCH_2N). Anal. Calcd: C, 29.81; H, 2.33; N, 9.27; S, 10.61. Found: C, 29.90; H, 2.31; N, 9.16; S, 10.66. FAB-MS ([M]+): m/z 459.1 ([**1b** −1PF_6^-]$^+$).

General Procedure for the Synthesis of Iron(II) Complexes. A solution of imidazolium hexafluorophosphate (262 μmol) in 3 mL of acetonitrile was slowly added to a suspension of [Fe{N(SiMe$_3$)$_2$}$_2$·THF] (118 mg, 262 μmol) in acetonitrile (3 mL) at −35 °C via a transfer cannula and gently warmed to room temperature. After stirring for 2 h, the deep-red solution was evaporated to dryness, the residue was redissolved in acetonitrile (2 mL), and the solution again was evaporated to remove residual amine. Next, the residue was dissolved in acetonitrile (1 mL) and diethyl ether was added, giving an orange-brown precipitate. The suspension was filtered via a filter

dx.doi.org/10.1021/ic500959m | *Inorg. Chem.* 2014, 53, 9598−9606

cannula, and to the red filtrate was added more diethyl ether until an orange precipitate formed. The supernatant solution was decanted, and the remaining orange solid was dried in vacuo.

*Tetrakis(acetonitrile)-cis-[bis(o-imidazol-2-ylidenefuran)-methane]iron(II) Hexafluorophosphate (**2a**).* The product is obtained as a bright-orange solid in 47% yield. ^{1}H NMR (400 MHz, CD_3CN, 300 K): δ 7.66 (d, $^{3}J_{HH}$ = 2.1 Hz, 2H, H_{im}), 7.56 (s, 2H, H_{Fu}), 7.47 (d, $^{3}J_{HH}$ = 2.0 Hz, 2H, H_{im}), 6.65 (virt. t, $^{3}J_{HH}$ = 2 Hz, 2H, H_{Fu}), 6.48 (d, $^{3}J_{HH}$ = 3.4 Hz, 2H, H_{Fu}), 6.17 (s, 2H, NCH_2N). $^{13}C\{^{1}H\}$ NMR (101 MHz, CD_3CN, 300 K): δ 196.06 ($NC_{Fe}N$), 145.89 (NCO), 142.02 (C*C*HCH), 128.62 (C_{im}), 124.73 (C_{im}), 112.73 (CH*C*HCH), 107.28 (CH*C*HO), 63.01 (NCH_2N). Anal. Calcd: C, 34.96; H, 3.06; N, 14.18. Found: C, 35.34; H, 3.13; N, 14.48.

*Tetrakis(acetonitrile)-cis-[bis(o-imidazol-2-ylidenethiophene)-methane]iron(II) Hexafluorophosphate (**2b**).* The product is obtained as a dark-orange solid in 56% yield. ^{1}H NMR (400 MHz, CD_3CN, 300 K): δ 7.64 (d, $^{3}J_{HH}$ = 2.2 Hz, 2H, H_{im}), 7.48 (dd, $^{3}J_{HH}$ = 5.6 Hz, $^{4}J_{HH}$ = 1.6 Hz, 2H, H_{Th}), 7.43 (d, $^{3}J_{HH}$ = 2.1 Hz, 2H, H_{im}), 7.19 (dd, $^{3}J_{HH}$ = 3.7 Hz, $^{4}J_{HH}$ = 1.6 Hz, 2H, H_{Th}), 7.10 (dd, $^{3}J_{HH}$ = 5.6 Hz, $^{3}J_{HH}$ = 3.7 Hz, 2H, H_{Th}), 6.14 (s, 2H, NCH_2N). $^{13}C\{^{1}H\}$ NMR (101 MHz, CD_3CN, 300 K): δ 192.85 ($NC_{Fe}N$), 141.83 (NCS), 130.12 (C*C*HCH), 128.68 (C_{im}), 126.83 (C_{im}), 126.53 (CH*C*HCH), 124.48 (CH*C*HS), 63.16 (NCH_2N). Anal. Calcd: C, 33.51; H, 3.18; N, 13.59; S, 7.78. Found: C, 33.39; H, 3.39; N, 13.51; S, 7.85.

■ ASSOCIATED CONTENT

Ⓢ Supporting Information

X-ray crystallographic data in CIF format (CCDC 997386−997389), DFT-optimized geometries of mono-PMe_3 derivatives of **2a** as *xyz* coordinates, ORTEP representation of the complex $[Fe(dmpe)_2(MeCN)_2]$, and additional ^{1}H, ^{13}C, ^{31}P, and HMQC 2D NMR spectra. This material is available free of charge via the Internet at http://pubs.acs.org.

■ AUTHOR INFORMATION

Corresponding Author

*Tel: +49 89 289 13096. E-mail: fritz.kuehn@ch.tum.de.

Notes

The authors declare no competing financial interest.

■ ACKNOWLEDGMENTS

The authors gratefully acknowledge support and funding from the KAUST, the EU project Next-GTL, and the Technische Universitat München Graduate School. J.R. thanks the Studienstiftung des deutschen Volkes for financial support.

■ REFERENCES

(1) (a) Öfele, K. *J. Organomet. Chem.* **1968**, *12*, P42−P43. (b) Wanzlick, H.-W.; Schönherr, H.-J. *Angew. Chem.* **1968**, *80*, 154. (c) Arduengo, A. J.; Davidson, F.; Dias, H. V. R.; Goerlich, J. R.; Khasnis, D.; Marshall, W. J.; Prakasha, T. K. *J. Am. Chem. Soc.* **1997**, *119*, 12742−12749.

(2) (a) Herrmann, W. A. *Angew. Chem., Int. Ed.* **2002**, *41*, 1290−1309. (b) Würtz, S.; Glorius, F. *Acc. Chem. Res.* **2008**, *41*, 1523−1533. (c) Díez-González, S.; Marion, N.; Nolan, S. P. *Chem. Rev.* **2009**, *109*, 3612−3676. (d) Lin, J. C. Y.; Huang, R. T. W.; Lee, C. S.; Bhattacharyya, A.; Hwang, W. S.; Lin, I. J. B. *Chem. Rev.* **2009**, *109*, 3561−3598. (e) Martin, D.; Melaimi, M.; Soleilhavoup, M.; Bertrand, G. *Organometallics* **2011**, *30*, 5304−5313.

(3) Ingleson, M. J.; Layfield, R. A. *Chem. Commun.* **2012**, *48*, 3579−3589.

(4) Liddle, S. T.; Edworthy, I. S.; Arnold, P. L. *Chem. Soc. Rev.* **2007**, *36*, 1732.

(5) Lavallo, V.; Grubbs, R. H. *Science.* **2009**, *326*, 559−562.

(6) (a) Day, B. M.; Pugh, T.; Hendriks, D.; Guerra, C. F.; Evans, D. J.; Bickelhaupt, F. M.; Layfield, R. A. *J. Am. Chem. Soc.* **2013**, *135*, 13338−13341. (b) Pugh, T.; Layfield, R. A. *Dalton Trans.* **2014**, *43*, 4251.

(7) (a) Öfele, K. *Angew. Chem.* **1969**, *81*, 936. (b) Huttner, G.; Gartzke, W. *Chem. Ber.* **1972**, *105*, 2714−2725. (c) Öfele, K.; Kreiter, C. G. *Chem. Ber.* **1972**, *105*, 529−540. (d) Bézier, D.; Sortais, J.-B.; Darcel, C. *Adv. Synth. Catal.* **2013**, *355*, 19−33.

(8) Riener, K.; Haslinger, S.; Raba, A.; Högerl, M. P.; Cokoja, M.; Herrmann, W. A.; Kühn, F. E. *Chem. Rev.* **2014**, *114*, 5215−5272.

(9) Danopoulos, A. A.; Tsoureas, N.; Wright, J. A.; Light, M. E. *Organometallics* **2004**, *23*, 166−168.

(10) (a) Liu, B.; Zhang, Y.; Xu, D.; Chen, W. *Chem. Commun.* **2011**, *47*, 2883−2885. (b) Grohmann, C.; Hashimoto, T.; Fröhlich, R.; Ohki, Y.; Tatsumi, K.; Glorius, F. *Organometallics* **2012**, *31*, 8047−8050. (c) Thagfi, J. A.; Lavoie, G. G. *Organometallics* **2012**, *31*, 7351−7358. (d) Kaufhold, O.; Hahn, F. E.; Pape, T.; Hepp, A. *J. Organomet. Chem.* **2008**, *693*, 3435−3440. (e) Zhang, Y.; Liu, B.; Wu, H.; Chen, W. *Chin. Sci. Bull.* **2012**, *57*, 2368−2376. (f) Smith, J. M.; Long, J. R. *Inorg. Chem.* **2010**, *49*, 11223−11230. (g) Klawitter, I.; Meyer, S.; Demeshko, S.; Meyer, F. *Z. Naturforsch.* **2013**, *68b*, 458. (h) Chen, M.-Z.; Sun, H.-M.; Li, W.-F.; Wang, Z.-G.; Shen, Q.; Zhang, Y. *J. Organomet. Chem.* **2006**, *691*, 2489−2494. (i) Wang, Y.; Sun, H.; Tao, X.; Shen, Q.; Zhang, Y. *Chin. Sci. Bull.* **2007**, *52*, 3193−3199. (j) Ouyang, Z.; Deng, L. *Organometallics* **2013**, *32*, 7268−7271.

(11) Al Thagfi, J.; Lavoie, G. G. *Organometallics* **2012**, *31*, 2463−2469.

(12) Kaplan, H. Z.; Li, B.; Byers, J. A. *Organometallics* **2012**, *31*, 7343−7350.

(13) Liu, B.; Xia, Q.; Chen, W. *Angew. Chem., Int. Ed.* **2009**, *48*, 5513−5516.

(14) Raba, A.; Cokoja, M.; Ewald, S.; Riener, K.; Herdtweck, E.; Pöthig, A.; Herrmann, W. A.; Kühn, F. E. *Organometallics* **2012**, *31*, 2793−2800.

(15) (a) Kück, J. W.; Raba, A.; Markovits, I. I. E.; Cokoja, M.; Kühn, F. E. *ChemCatChem.* **2014**, *6*, 1882−1886. (b) Raba, A.; Cokoja, M.; Herrmann, W. A.; Kühn, F. E. *Chem. Commun.* **2014**, DOI: 10.1039/C4CC02178A.

(16) Xi, Z.; Zhang, X.; Chen, W.; Fu, S.; Wang, D. *Organometallics* **2007**, *26*, 6636−6642.

(17) Zhu, L.; Guo, P.; Li, G.; Lan, J.; Xie, R.; You, J. *J. Org. Chem.* **2007**, *72*, 8535−8538.

(18) Zhang, H.; Cai, Q.; Ma, D. *J. Org. Chem.* **2005**, *70*, 5164−5173.

(19) Xi, Z.; Liu, F.; Zhou, Y.; Chen, W. *Tetrahedron* **2008**, *64*, 4254−4259.

(20) (a) Kreisel, K. A.; Yap, G. P. A.; Theopold, K. H. *Organometallics* **2006**, *25*, 4670−4679. (b) Meyer, S.; Demeshko, S.; Dechert, S.; Meyer, F. *Inorg. Chim. Acta* **2010**, *363*, 3088−3092.

(21) Meyer, S.; Klawitter, I.; Demeshko, S.; Bill, E.; Meyer, F. *Angew. Chem., Int. Ed.* **2013**, *52*, 901−905.

(22) Danopoulos, A. A.; Braunstein, P.; Stylianides, N.; Wesolek, M. *Organometallics* **2011**, *30*, 6514−6517.

(23) Danopoulos, A. A.; Tsoureas, N.; Wright, J. A.; Light, M. E. *Organometallics* **2004**, *23*, 166−168.

(24) Mercs, L.; Neels, A.; Albrecht, M. *Dalton Trans.* **2008**, 5570−5576.

(25) Morvan, D.; Capon, J.-F.; Gloaguen, F.; Pétillon, F. Y.; Schollhammer, P.; Talarmin, J.; Yaouanc, J.-J.; Michaud, F.; Kervarec, N. *J. Organomet. Chem.* **2009**, *694*, 2801−2807.

(26) Meyer, S.; Orben, C. M.; Demeshko, S.; Dechert, S.; Meyer, F. *Organometallics* **2011**, *30*, 6692−6702.

(27) Zlatogorsky, S.; Muryn, C. A.; Tuna, F.; Evans, D. J.; Ingleson, M. J. *Organometallics* **2011**, *30*, 4974−4982.

(28) Britovsek, G. J. P.; Gibson, V. C.; Hoarau, O. D.; Spitzmesser, S. K.; White, A. J. P.; Williams, D. J. *Inorg. Chem.* **2003**, *42*, 3454−3465.

(29) Cramer, S. A.; Jenkins, D. M. *J. Am. Chem. Soc.* **2011**, *133*, 19342−19345.

(30) Blom, B.; Tan, G.; Enthaler, S.; Inoue, S.; Epping, J. D.; Driess, M. *J. Am. Chem. Soc.* **2013**, *135*, 18108−18120.

(31) George, A. V.; Field, L. D.; Malouf, E. Y.; McQueen, A. E. D.; Pike, S. R.; Purches, G. R.; Hambley, T. W.; Buys, I. E.; White, A. H.;

Hockless, D. C. R.; Skelton, B. W. *J. Organomet. Chem.* **1997**, *538*, 101−110.
(32) (a) Andersen, R. A.; Faegri, K.; Green, J. C.; Haaland, A.; Lappert, M. F.; Leung, W. P.; Rypdal, K. *Inorg. Chem.* **1988**, *27*, 1782−1786. (b) Olmstead, M. M.; Power, P. P.; Shoner, S. C. *Inorg. Chem.* **1991**, *30*, 2547−2551.
(33) Keegstra, M. A.; Klomp, A. J. A.; Brandsma, L. *Synth. Commun.* **1990**, *20*, 3371−3374.
(34) Zhu, L.; Guo, P.; Li, G.; Lan, J.; Xie, R.; You, J. *J. Org. Chem.* **2007**, *72*, 8535−8538.
(35) Frisch, M. J.; et al. *Gaussian 09*; Gaussian, Inc.: Wallingford, CT, 2009.
(36) (a) Lee, C.; Yang, W.; Parr, R. G. *Phys. Rev. B* **1988**, *37*, 785−789. (b) Becke, A. D. *J. Chem. Phys.* **1993**, *98*, 5648−5652.
(37) (a) Ditchfield, R.; Hehre, W. J.; Pople, J. A. *J. Chem. Phys.* **1971**, *54*, 724−728. (b) Hehre, W. J.; Ditchfield, R.; Pople, J. A. *J. Chem. Phys.* **1972**, *56*, 2257−2261. (c) Francl, M. M.; Pietro, W. J.; Hehre, W. J.; Binkley, J. S.; Gordon, M. S.; DeFrees, D. J.; Pople, J. A. *J. Chem. Phys.* **1982**, *77*, 3654−3665.
(38) Scalmani, G.; Frisch, M. J. *J. Chem. Phys.* **2010**, *132*, 114110.
(39) (a) Wachters, A. J. H. *J. Chem. Phys.* **1970**, *52*, 1033−1036. (b) Hay, P. J. *J. Chem. Phys.* **1977**, *66*, 4377−4384. (c) Krishnan, R.; Binkley, J. S.; Seeger, R.; Pople, J. A. *J. Chem. Phys.* **1980**, *72*, 650−654. (d) McLean, A. D.; Chandler, G. S. *J. Chem. Phys.* **1980**, *72*, 5639−5648. (e) Raghavachari, K.; Trucks, G. W. *J. Chem. Phys.* **1989**, *91*, 1062−1065.
(40) *APEX 2, suite of crystallographic software*, version 2008.4; Bruker AXS Inc.: Madison, WI, 2008.
(41) *SAINT*, version 7.56a, and *SADABS*, version 2008/1; Bruker AXS Inc.: Madison, WI, 2008.
(42) (a) Sheldrick, G. M. *Acta Crystallogr., Sect. A* **1998**, *64*, 112−122. (b) Hübschle, C. B.; Sheldrick, G. M.; Dittrich, B. *J. Appl. Crystallogr.* **2011**, *44*, 1281−1284.
(43) Wilson, A. J. C. *International Tables for Crystallography*; Kluwer Academic Publishers: Dordrecht, The Netherlands, 1992; Vol. *C*, Tables 6.1.1.4, 4.2.6.8, and 4.2.4.2, pp 500−502, 219−222, and 193−199.
(44) Spek, A. L. *PLATON, A Multipurpose Crystallographic Tool*; Utrecht University: Utrecht, The Netherlands, 2010.